Information Technology, Artificial Intelligence and Machine Learning in Smart Grid – Performance Comparison between Topology Identification Methodology and Neural Network Identification Methodology for the Branch Number Approximation of Overhead Low-Voltage Broadband over Power Lines Network Topologies

Athanasios G. Lazaropoulos[1,2,*]

1: School of Electrical and Computer Engineering / National Technical University of Athens / 9 Iroon Polytechniou Street / Zografou, GR 15780
2: Department of Industrial Design and Production Engineering / School of Engineering / University of West Attica / 250 Thivon & P. Ralli / Athens, GR 12244

Broadband over Power Lines (BPL) networks that are deployed across the smart grid can benefit from the usage of machine learning, as smarter grid diagnostics are collected and analyzed. In this paper, the neural network identification methodology of Overhead Low-Voltage (OV LV) BPL networks that aims at identifying the number of branches for a given OV LV BPL topology channel attenuation behavior is proposed, which is simply denoted as NNIM-BNI. In order to identify the branch number of an OV LV BPL topology through its channel attenuation behavior, NNIM-BNI exploits the Deterministic Hybrid Model (DHM), which has been extensively tested in OV LV BPL networks for their channel attenuation determination, and the OV LV BPL topology database of Topology Identification Methodology (TIM). The results of NNIM-BNI towards the branch number identification of OV LV BPL topologies are compared against the ones of a newly proposed TIM-based methodology, denoted as TIM-BNI.

1. Introduction

The evolution of the today's traditional power grid hastens the coexistence of this grid with an intelligent IP-based communications network enhanced with a plethora of broadband applications, which is widely referred to as the smart grid [1-5]. Broadband over Power Lines (BPL) technology lies among the available communications alternatives that may support the required information flow of smart grid. The two strongest points of BPL networks compared to the other communications

solutions, such as Radio Frequency (RF) mesh, modified Long Term Evolution (LTE), Code Division Multiple Access (CDMA) at sub GHz bands, dedicated fiber along transmission / distribution lines and 5G communications, are: (i) their easiness to support a communications channel upon the already installed wired power grid infrastructure, and (ii) their interoperability with the aforementioned communications solutions by exploiting the BPL wireline / wireless interfaces [6-10].

Since BPL networks are deployed upon the wired power grid infrastructure that is not a transmission medium designed for communications signals, BPL signals are subjected to various inherent deficiencies, such as high and frequency-selective channel attenuation and noise [11-19]. As the modeling of signal transmission and propagation across BPL channels is concerned, a variety of BPL channel models has been proposed in the literature. BPL channels may follow either a deterministic approach or a statistical approach or a bottom-up approach or a top-down approach or appropriate syntheses of the aforementioned approaches [5], [11-14], [20-36]. Among the available state-of-art BPL channel models of the literature, the deterministic hybrid model (DHM) has extensively been employed to describe the channel behavior of various multiconductor transmission line (MTL) configurations in transmission and distribution BPL network topologies and is also adopted in this paper [11-14], [20], [23], [25, 26], [30]. The outputs of DHM, such as channel attenuation and capacity, are crucial broadband performance metrics of the BPL topologies that further act as the big data feed for the supported broadband applications of smart grid, like Fault and Instability Identification Methodology (FIIM) [3], [37], Main Line Fault Localization Methodology (MLFLM) [4], Topology Identification Methodology (TIM) [3], [38], etc. As TIM is applied in this paper, TIM is considered to be among the most useful piecewise monotonic data approximation (PMA) broadband applications and approximates the exact topological characteristics (*i.e.*, number of branches, length of branches, length of main lines and branch terminations) of an examined BPL topology by exploiting channel attenuation measurements of the examined BPL topology and TIM BPL topology database. In fact, the OV LV BPL topology database of TIM that is used in this paper assigns topological characteristics to respective channel attenuation measurements for a myriad of OV LV BPL topologies. Although there is the great number of OV LV BPL topologies in the TIM OV LV BPL topology database, a TIM-based methodology is proposed here, which exploits channel attenuation measurements and is denoted as TIM-BNI. The purpose is to approximate the number of branches when the OV LV BPL topology with known channel attenuation measurements is not among the OV LV BPL topologies of the TIM OV LV BPL topology database.

As already been mentioned, the leading philosophy behind the BPL channel characterization literature concentrates on following either a deterministic approach or a statistical approach or a bottom-up approach or a top-down approach or appropriate syntheses of the aforementioned approaches, but artificial intelligence (AI) and machine learning (ML) aspire to derive the input-output relations of the BPL channels by learning and capturing information from big data such as those stored in TIM OV LV BPL topology database [39-41]. Among the available AI and ML schemes, neural networks are chosen in this paper due to: (i) their popularity in the communications research field; (ii) their ease of implementation in various architectures; and (iii) their ability to be trained through the backpropagation learning process [42, 43]. By exploiting the available big data of the TIM OV LV BPL topology database and the backpropagation learning process, neural networks are going to be deployed in order to

discover BPL system properties and provide crucial broadband performance metrics for the BPL topologies in the future by deriving relations and revealing hidden states among the BPL system phenomena [40], [44]. Hence, the portfolio of the available supported BPL broadband applications of smart grid is enriched in this paper with the proposed neural network identification methodology for the branch number identification (NNIM-BNI); more specifically, NNIM-BNI of OV LV BPL topologies aims at approximating the number of branches for a given OV LV BPL topology channel attenuation behavior when NNIM-BNI ignores the topological characteristics of the examined OV LV BPL topology. Similarly to the TIM-BNI, NNIM-BNI is going to approximate the number of branches when the OV LV BPL topology, whose channel attenuation measurements are considered, is not among the OV LV BPL topologies of the TIM OV LV BPL topology database. The approximation performances of the two proposed branch number identification methodologies of this paper, *i.e.*, TIM-BNI and NNIM-BNI, are going to be assessed and compared for indicative OV LV BPL topologies that lie outside the TIM OV LV BPL topology database when different operation settings are examined.

The rest of this paper is organized as follows: Section 2 briefly presents the OV LV MTL configurations and the indicative OV LV BPL topologies that are going to be used during the benchmark process of this paper. Also, this Section summarizes the basics of DHM and TIM. Section 3 initially describes TIM-BNI as well as the corresponding performance metrics for its evaluation. Then, a brief description of neural networks is given, while NNIM-BNI with its corresponding performance metrics is also demonstrated. Section 4 presents the performance metrics results for TIM-BNI and NNIM-BNI for the indicative OV LV BPL topologies when different operation settings are assumed. Section 5 concludes this paper.

2. OV LV MTL Configurations, Indicative OV LV BPL Topologies, DHM and TIM and TIM-BNI

In this Section, the basics concerning the propagation and transmission of BPL signals across the OV LV power grid are first given. More specifically, OV LV MTL configurations and the indicative OV LV BPL topologies, which are going to be used for the assessment of TIM-BNI and NNIM-BNI, are presented. Then, the channel model of DHM is briefly analyzed by focusing on its main output of the channel attenuation of OV LV BPL topologies, which is of interest in this paper. Since the topological characteristics and the channel attenuation of OV LV BPL topologies are well defined, TIM and TIM OV LV BPL topology database are demonstrated.

2.1 OV LV MTL Configurations and Indicative OV LV BPL Topologies

In accordance with [45], the typical OV LV MTL configuration that is examined in this paper is illustrated in Fig. 1(a). The examined OV LV MTL configuration consists of four parallel non-insulated conductors (i.e., $n^{OVLV} = 4$), which are spaced each other by a vertical distance Δ_{OVLV}. The upper conductor is the neutral conductor with a radius of $r_{OVLV,n}$, while the lower three conductors are the three LV phases, each with a radius of $r_{OVLV,p}$. The lowest phase conductor is hung at the height h_{OVLV} above the ground, which is considered to be the reference conductor of the OV LV MTL configuration.
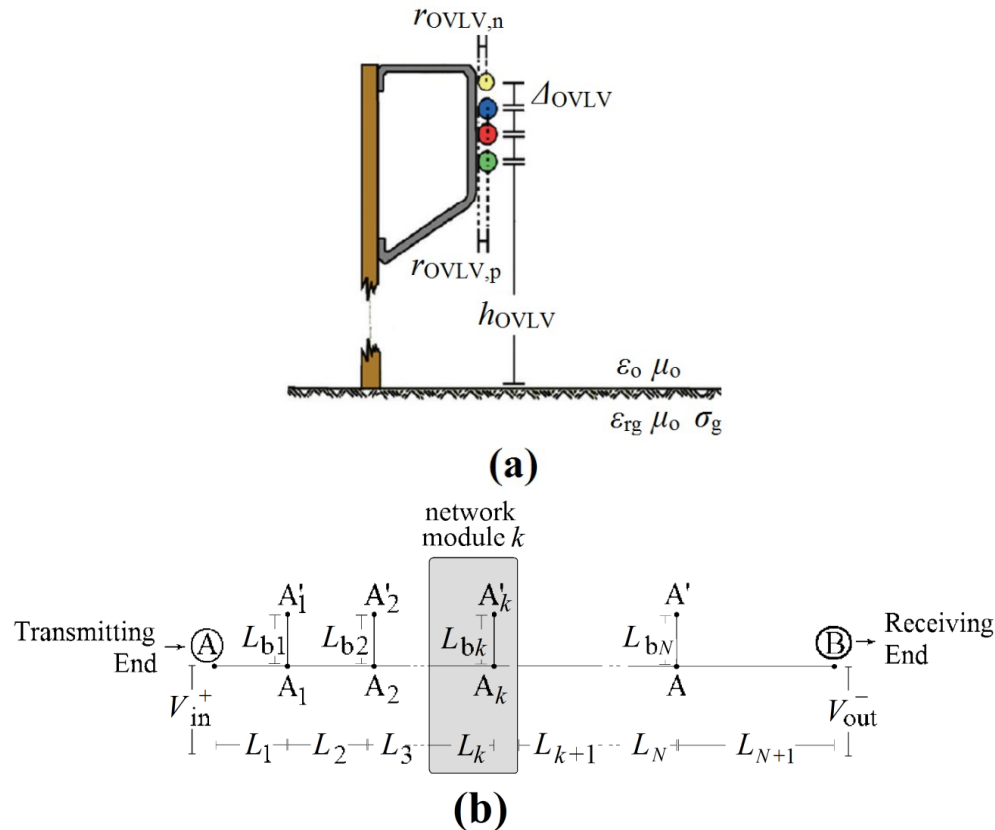
Fig. 1. (a) OV LV MTL configuration [20], [45]. Typical OV LV BPL topology with N branches [36].

The exact dimensions, the material of the conductors, the structure of the conductors and the properties of the imperfect lossy ground are reported in [11], [20], [23], [45-47], while their impact on the BPL signal propagation has been analyzed in [48-50].

To further study the BPL signal transmission across the OV LV BPL network, each network may be divided into cascaded OV LV BPL topologies bounded by the transmitting and receiving ends, while a generic OV LV BPL topology is illustrated in Fig. 1(b). Across the BPL signal transmission path, N branches with their respective terminations, which are assumed to be open-circuit terminations in this paper, may be encountered. The arbitrary k, $k=1,…,N$ branch has length equal to L_{bk} and is located at distance $\sum_{i=1}^{k} L_i$ from the transmitting end. The typical length $\sum_{i=1}^{N+1} L_i$ of 1000 m is assumed between the transmitting and receiving ends.

In accordance with the literature [9], [20], five indicative OV LV BPL topologies (*i.e.*, LOS, rural, suburban, urban A and urban B) are usually used, so that a general study of all OV LV BPL topology classes may be fulfilled. In Table 1, these five indicative OV LV BPL topologies are reported in terms of their topological characteristics and their branch number that is a parameter of interest in this paper. More specifically, the four indicative OV LV BPL topologies shown in green background color in Table 1 (*i.e.*, urban case A, suburban case, rural case and LOS case) are going to be further adopted, so that the approximation performances of the two proposed branch number identification methodologies of this paper, say, NNIM-BNI and TIM-BNI

Table 1
Indicative OV LV BPL Topologies

OV LV BPL Topology Name	Branch Number (N)	Length of Main Lines	Length of Branches
Urban case A (Typical urban case)	3	L_1=500m, L_2=200m, L_3=100m, L_4=200m	L_{b1}=8m, L_{b2}=13m, L_{b3}=10m
Urban case B (Aggravated urban case)	5	L_1=200m, L_2=50m, L_3=100m, L_4=200m, L_5=300m, L_6=150m	L_{b1}=12m, L_{b2}=5m, L_{b3}=28m, L_{b4}=41m, L_{b5}=17m
Suburban case	2	L_1=500m, L_2=400m, L_3=100m	L_{b1}=50m, L_{b2}=10m
Rural case	1	L_1=600m, L_2=400m	L_{b1}=300m
Line-of-Sight (LOS) case	0	L_1=1000m	-

may be assessed. Note that: (i) the urban case A, suburban case and rural case will be excluded from the TIM OV LV BPL topology database, so that NNIM-BNI and TIM-BNI blindly approximate their branch numbers; (ii) The LOS case is included in the TIM OV LV BPL topology database, because it is unique. Note that there can be no blind approximation by NNIM-BNI and TIM-BNI in the LOS case and for that reason is examined for verification issues; and (iii) The urban case B of 5 branches has been excluded for a further examination due to the high delay that imposes to the TIM OV LV BPL topology database preparation.

2.2 DHM and TIM

DHM can be considered to be a synthetic BPL channel model where a fine module concatenation of a bottom-up, a top-down, a coupling scheme and other performance metric computation modules occurs [9], [11-14], [20], [45]. By the interconnection of the first two DHM modules (*i.e.*, the bottom-up and the top-down module), the propagation and transmission problem of the BPL signal across an OV LV BPL topology for a given OV LV MTL configuration is well defined, thus permitting the computation of the line channel transfer function matrix $\mathbf{H}^{OVLV}\{\cdot\}$, since more than 2 conductors are encountered in the OV LV MTL configuration of interest. Actually, the $n^{OVLV} \times n^{OVLV}$ line channel transfer function matrix $\mathbf{H}^{OVLV}\{\cdot\}$ that relates line quantities with modal ones is given by

$$\mathbf{H}^{OVLV}\{\cdot\} = \mathbf{T}_V^{OVLV} \cdot \mathbf{H}^{OVLV,m}\{\cdot\} \cdot \left(\mathbf{T}_V^{OVLV}\right)^{-1} \qquad (1)$$

where $\mathbf{H}^{OVLV,m}\{\cdot\}$ is the $n^{OVLV} \times n^{OVLV}$ modal channel transfer function matrix that mainly depends on the examined OV LV MTL configuration and OV LV BPL topology, and $\mathbf{T}_V^{OVLV}$ is a $n^{OVLV} \times n^{OVLV}$ transformation matrix that depends on the physical properties of the MTLs and the geometry of the OV LV MTL configuration. Since modal channel transfer function and transformation matrices are frequency dependent, this implies that the line channel transfer function is also a frequency dependent parameter. On the basis of the first two DHM modules, the third DHM module arranges the way that the BPL signals are injected into and extracted from the TLs of the MTL configurations; say, the third DHM module mathematically describes the different coupling schemes of the BPL signal injection / extraction [51, 52]. With reference to eq. (1), the coupling

scheme channel transfer function, which is the mathematical expression of the interconnections of the first three DHM modules relating output BPL signals and input ones is given by

$$H^{OVLV,C}\{\cdot\} = [\mathbf{C}^{out}]^{OVLV,C} \cdot \mathbf{H}^{OVLV}\{\cdot\} \cdot [\mathbf{C}^{in}]^{OVLV,C} \qquad (2)$$

for given coupling scheme where $[\cdot]^c$ denotes the applied coupling scheme, $\mathbf{C}^{in}$ is the input coupling $n^{OVLV} \times 1$ column vector dealing with the BPL signal injection process and $\mathbf{C}^{out}$ is the ouput coupling $1 \times n^{OVLV}$ line vector dealing with the BPL signal extraction process. More details concerning the available coupling schemes and the respective involved conductors of the examined OV LV MTL configuration are detailed in [51, 52]. Other DHM performance metric computation modules are outside the scope of this paper and are not further analyzed here. It is evident from eq. (2) that the coupling scheme channel transfer function is a frequency dependent parameter and depends on the topological characteristics of the examined OV LV BPL topology. Thus, for given OV LV MTL configuration and coupling scheme, their corresponding coupling scheme channel transfer functions can be computed by DHM by only adjusting the topological characteristics of OV LV BPL topologies.

The aforementioned collection of topological characteristics and corresponding coupling scheme channel transfer functions for a variety of OV LV BPL topologies may act as the big data feed of the supported smart grid broadband applications, such as TIM of this paper [3], [38]. In accordance with [3], TIM can identify an OV LV BPL topology with respect to its topological characteristics (*i.e.*, number of branches, length of branches, length of main distribution lines and branch terminations) when its corresponding coupling scheme transfer function behavior is known. In fact, by appropriately storing and retrieving the previous collection of OV LV BPL topologies to / from the TIM OV LV BPL topology database, TIM can identify an OV LV BPL topology even if significant measurement differences may occur by appropriately exploiting piecewise monotonic data approximations [53, 54]. As the TIM OV LV BPL topology database is concerned in this paper, no measurement differences are assumed. Depending on the examined scenario of accuracy degree, corresponding TIM OV LV BPL topology database specifications can be assumed for the database preparation; say, the maximum number of branches N_{max}, the length spacing L_s for both branch distance and branch length, and the maximum branch length $L_{b,max}$ for the OV LV BPL topologies that are going to be stored in the database. Finally, for each OV LV BPL topology of the TIM OV LV BPL topology database, the following data are maintained for the further analysis of this paper: (i) its ID number p in the TIM OV LV BPL topology database when P is the number of all OV LV BPL topologies in the TIM OV LV BPL topology database; (ii) the actual number of branches N; and (iii) the coupling scheme channel transfer function values with respect to the frequency.

3. TIM-BNI and NNIM-BNI

In this Section, the proposal of TIM-BNI and NNIM-BNI is theoretically detailed. Suitable performance metrics, which allow the approximation assessment of the branch numbers of the indicative OV LV BPL topologies in each methodology, are reported. Note that prior to the presentation of NNIM-BNI, an introduction of neural networks in OV LV BPL networks is also given.

3.1 TIM-BNI

With reference to Sec. 2.2, the TIM OV LV BPL topology database may consist of a plethora of OV LV BPL topologies whose number depends on the required accuracy degree or, in other words, the TIM OV LV BPL topology database specifications applied (*i.e.*, the maximum number of branches N_{max}, the length spacing L_s for both branch distance and branch length and the maximum branch length $L_{b,max}$, operation frequency range, etc). Since indicative OV LV BPL topologies of Table 1 are not included in the TIM OV LV BPL topology database by definition except LOS case, TIM-BNI is going to approximate the branch number of the examined indicative OV LV BPL topology by comparing its coupling scheme channel transfer function values with respect to the frequency, which are known for the branch number identification problem of this paper, against the respective ones of all the OV LV BPL topologies of the TIM OV LV BPL topology database. To identify the OV LV BPL topologies of the TIM OV LV BPL topology database that better approximate the channel attenuation behavior of the examined indicative OV LV BPL topology, the performance metric of the root-mean-square deviation (RMSD) of the amplitude of coupling scheme channel transfer functions in dB is first going to be computed as follows:

$$RMSD_{\text{TIM}-\text{BNI},p} = \sqrt{\frac{\sum_{q=1}^{Q}\left(\left|H_{\text{TIM},p}^{\text{OVLV,C}}(f_q)\right|_{\text{dB}} - \left|H_{\text{indicative}}^{\text{OVLV,C}}(f_q)\right|_{\text{dB}}\right)^2}{Q}} \qquad (3)$$

where

$$f_q = 3\text{MHz} + (q-1)\cdot f_s, q = 1, \dots, Q \qquad (4)$$

is the flat-fading subchannel start frequency, f_s is the flat-fading subchannel frequency spacing, Q is the number of subchannels in the examined frequency range, $H_{\text{indicative}}^{\text{OVLV,C}}\left(f_q\right)$ is the coupling scheme channel transfer function of the indicative OV LV BPL topology at frequency f_q and $H_{\text{TIM},p}^{\text{OVLV,C}}\left(f_q\right)$ is the coupling scheme channel transfer function of the *p*-th OV LV BPL topology of the TIM OV LV BPL topology database at frequency f_q. The average value of the branch numbers of the *R* OV LV BPL topologies of the TIM OV LV BPL topology database that present the *R* lowest RMSDs among the *P* computed ones defines the TIM-BNI approximation of the branch number of the examined indicative OV LV BPL topology $N_{\text{TIM}-\text{BNI}}$. It is evident that the TIM-BNI performance towards the branch number identification of OV LV BPL topologies, that is numerically assessed in Section 4, is affected by the required accuracy degree of the TIM OV LV BPL topology database and the number *R* of the lowest RMSDs that are taken into account during the approximation.

3.2 Neural Networks and NNIM-BNI

As an application tool of the ML philosophy, neural networks can acquire knowledge and unveil hidden system properties or patterns from the simple output observations during the system operation. Neural networks have already been adopted in [55] for the channel attenuation determination of BPL networks. As already been mentioned, a main advantage of the neural networks is their ease of implementations in parallel on concurrent architectures [40], while neural networks become more accurate during their approximations as the backpropagation learning process exists [42, 43], [56].

In Fig. 2, the structure of the fully connected neural network with *HL* hidden layers of neurons that is adopted by NNIM-BNI in this paper is shown. More specifically,

this neural network receives as input the $Q \times 1$ column vector $\Delta \mathbf{H}_{\text{TIM},p,hl=0}^{\text{OVLV,C}}\{\cdot\}$ that is given by

$$\Delta \mathbf{H}_{\text{TIM},p,hl=0}^{\text{OVLV,C}}\{\cdot\} = [\,\left|H_{\text{TIM},p}^{\text{OVLV,C}}(f_1)\right|_{\text{dB}} - \left|H_{\text{LOS}}^{\text{OVLV,C}}(f_1)\right|_{\text{dB}} \cdots \left|H_{\text{TIM},p}^{\text{OVLV,C}}(f_q)\right|_{\text{dB}} - \left|H_{\text{LOS}}^{\text{OVLV,C}}(f_q)\right|_{\text{dB}} \cdots \left|H_{\text{TIM},p}^{\text{OVLV,C}}(f_Q)\right|_{\text{dB}} - \left|H_{\text{LOS}}^{\text{OVLV,C}}(f_Q)\right|_{\text{dB}}\,]^{\text{T}} \quad (5)$$

Note that the column vector $\Delta \mathbf{H}_{\text{TIM},p,hl=0}^{\text{OVLV,C}}\{\cdot\}$ concerns the arbitrary p-th OV LV BPL topology of the TIM OV LV BPL topology database at frequencies f_q, $q = 1, \ldots, Q$. In eq. (5), $\left|H_{\text{LOS}}^{\text{OVLV,C}}\{\cdot\}\right|_{\text{dB}}$ is the amplitude of the coupling scheme channel transfer functions of the LOS case of Table 1 in dB and $[\cdot]^{\text{T}}$ denotes the transpose of the matrix. After the input layer, the hidden layers occur. For the arbitrary hl hidden layer, its output $Q \times 1$ column vector $\Delta \mathbf{H}_{\text{TIM},p,hl}^{\text{OVLV,C}}\{\cdot\}$ is given by

$$\Delta \mathbf{H}_{\text{TIM},p,hl}^{\text{OVLV,C}}\{\cdot\} = \sigma\left(\mathbf{W}_{hl} \cdot \Delta \mathbf{H}_{\text{TIM},p,hl-1}^{\text{OVLV,C}}\{\cdot\} + \mathbf{b}_{hl}\right) \quad (6)$$

where $\sigma(\cdot)$ is the activation function, $\mathbf{W}_{hl}$ is the the $Q \times Q$ array of weights of the hl hidden layer and $\mathbf{b}_{hl}$ is the the $Q \times Q$ array of biases of the hl hidden layer. The output of the fully connected neural network that coincides with the output of the HL hidden layer is the NNIM-BNI approximation of the branch number of the examined indicative OV LV BPL topology $N_{\text{NNIM-BNI}}$.

Actually, NNIM-BNI exploits the MATLAB neural network training program of [43], [57] that is based on the architecture of the fully connected neural network demonstrated in Fig. 2. In accordance with [43], [57], NNIM-BNI is going to train neural networks of variable numbers of hidden layers by using the input and output data contained in the TIM OV LV BPL topology database with respect to eqs. (5) and (6). In accordance with [43], [57], NNIM-BNI is going to randomly split the supplied data of the OV LV BPL topologies of the TIM OV LV BPL topology database into three phase, *i.e.*, training, validation and testing. According to [43], [57], the Levenberg-Marquardt algorithm is adopted during the training phase of NNIM-BNI, while the performance metric of RMSD of the amplitude of the differences of coupling scheme channel transfer functions in dB as described in eq. (5) is computed for the OV LV BPL topologies of the TIM OV LV BPL topology database during the testing phase. In general terms, the parameters of the neural networks with smaller RMSDs per hidden layer are those that are selected for the testing where the four indicative OV LV BPL topologies of Table 1 are concerned. Hence, apart from the RMSD of the OV LV BPL topologies of the TIM OV LV BPL topology database selected for the testing phase, the MATLAB neural network training program of [43], [57] can also compute RMSD of the indicative OV LV BPL topologies for different numbers of the hidden layers. Therefore, NNIM-BNI gives the NNIM-BNI approximation value of the branch numbers $N_{\text{NNIM-BNI}}$ of the examined indicative OV LV BPL topologies as well as their approximation RMSDs for the aforementioned topologies per hidden layer as output. It is evident that the NNIM-BNI performance towards the branch number identification of OV LV BPL topologies, which is also numerically assessed in Section 4 in comparison with the TIM-BNI performance, is affected by the required accuracy degree of the TIM OV LV BPL topology database and the participation percentage of the three phases (*i.e.*, training, validation and testing) during the operation of its MATLAB neural network training program.
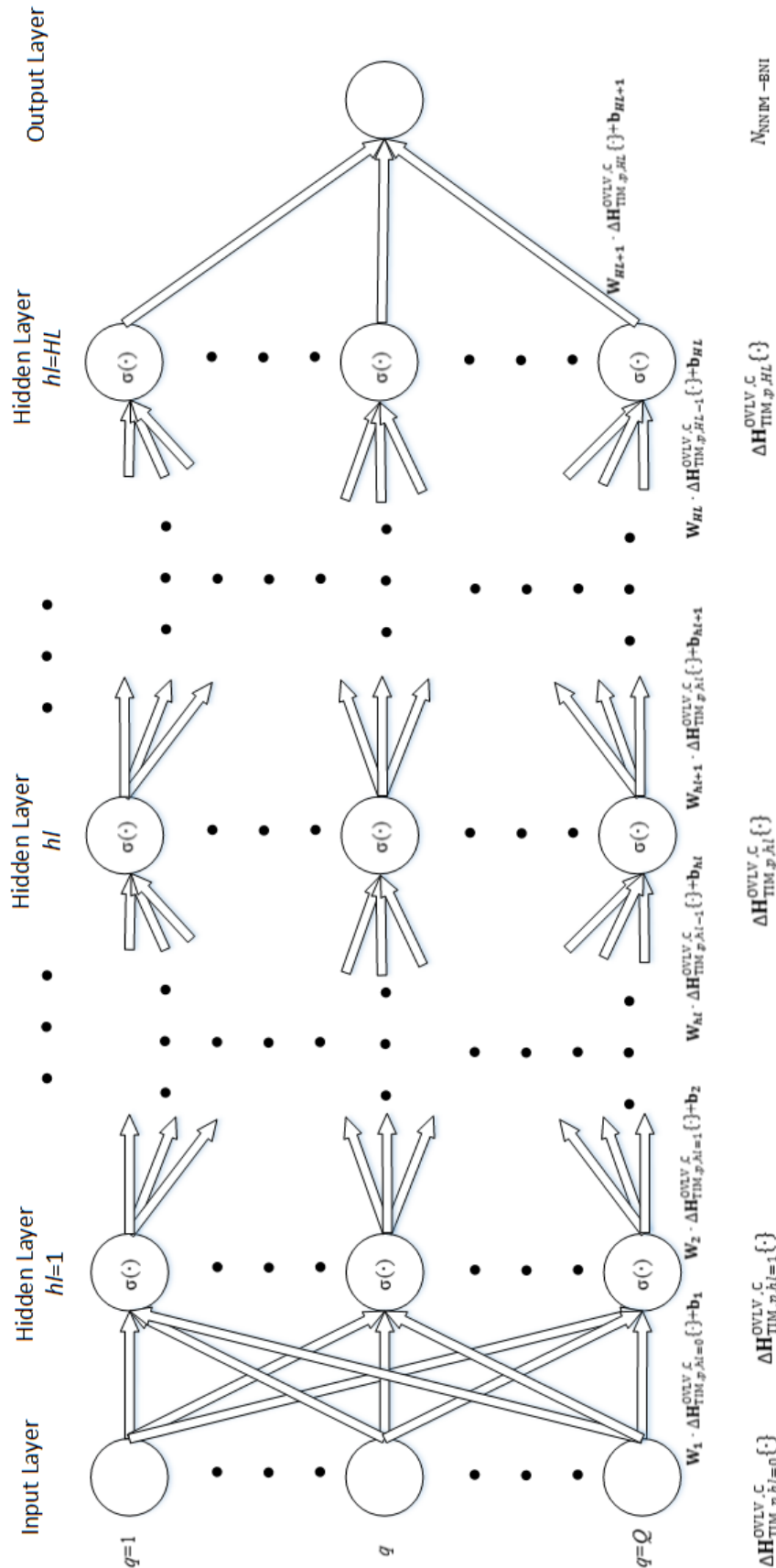
Fig. 2. Architecture of the fully connected neural network with *HL* hidden layers.

4. Numerical Results and Discussion

In this Section, numerical results concerning the performance of TIM-BNI and NNIM-BNI are presented as well as their comparison. On the basis of the default operation settings of the base scenario given in Sec.4.1, the performance metric of RMSD is applied in order to assess TIM-BNI and NNIM-BNI approximations. In Sec. 4.2, the impact of higher detail (*e.g.,* wider operation frequency range) during the preparation of the OV LV BPL topologies of the TIM OV LV BPL topology database is assessed when TIM-BNI and NNIM-BNI are applied. Also, the issue of the representativeness of the TIM OV LV BPL topology database is addressed. In Sec. 4.3, the role of the number of OV LV BPL topologies of the TIM OV LV BPL topology database that are considered during the computation of the average value of the branch numbers is investigated during the operation of TIM-BNI. In Sec. 4.4, the role of the participation percentages of the three phases (*i.e.*, training, validation and testing) during the operation of NNIM-BNI is examined.

4.1 Base Scenario and Default Operation Settings

As the base scenario of the cooperation of the TIM OV LV BPL topology database, TIM-BNI and NNIM-BNI are concerned, and the following default operation settings are assumed:

- As the preparation of the TIM OV LV BPL topology database is regarded, the OV LV MTL configuration of Fig. 1(a) and the typical OV LV BPL topology with *N* branches of Fig. 1(b) are assumed. On the basis of the required parameters of the TIM OV LV BPL topology database [3], [38], during the preparation of the TIM OV LV BPL topology database, its OV LV BPL topologies considered comprises from 0 (say "LOS" case) up to 3 branches in accordance with Sec. 2.1 and Table 1. The length spacings for branch distance and branch length are assumed to be equal to 100 m and 25 m, respectively, while the branch line length may range from 0 m to 100 m. Note that the distribution line length has already been assumed to be the typical one in Sec. 2.1 thus being equal to 1000 m. The frequency range is assumed equal to 3-30 MHz, while the flat-fading subchannel frequency spacing is equal to 1 MHz. For each OV LV BPL topology of the *P* ones of the TIM OV LV BPL topology database, its ID number *p* in the TIM OV LV BPL topology database, its number of branches, and the amplitude of its coupling scheme channel transfer function in dB with respect to the frequency are stored in the TIM OV LV BPL topology database.

- As the operation of the TIM-BNI is concerned, the performance metric of RMSD of the amplitudes of coupling scheme channel transfer functions in dB of the OV LV BPL topologies of the TIM OV LV BPL topology database with respect to the ones of each of the indicative OV LV BPL topologies of Table 1 is applied as described in eq. (3). For the base scenario where default operation settings are assumed, the average value of the branch numbers of the *R=5* OV LV BPL topologies of the TIM OV LV BPL topology database that presents the 5 lowest RMSDs among the *P* computed ones defines the TIM-BNI approximation of the branch number $N_{\text{TIM-BNI}}$ of each of the examined indicative OV LV BPL topologies of Table 1. For each of the examined indicative OV LV BPL topologies of Table 1, the TIM-BNI performance assessment is going to be fulfilled through the comparison between the TIM-BNI approximated branch

number value $N_{\text{TIM}-\text{BNI}}$ and the actual one while the performance metric of RMSD again assess the overall TIM-BNI approximation for the four examined indicative OV LV BPL topologies of Table 1.

- As the operation of the NNIM-BNI is concerned, NNIM-BNI is based on the MATLAB neural network training program of [43], [57]. In accordance with [43], [57], the division of the available OV LV BPL topologies of the TIM OV LV BPL topology database is random, while the default participation percentage of the three phases of the MATLAB neural network training program of [43] and [57] (*i.e.*, training, validation and testing) during the operation of NNIM-BNI are assumed to be equal to 70%, 15% and 15%, respectively. Given the amplitudes of coupling scheme channel transfer functions in dB for each of the four examined indicative OV LV BPL topologies of Table 1, NNIM-BNI gives the respective NNIM-BNI approximation of the branch numbers $N_{\text{NNIM}-\text{BNI}}$ per hidden layer as output, where the maximum number of hidden layers HL is assumed to be equal to 5. Since the behavior and performance of the machine learning algorithms and the neural network approaches are referred to as stochastic, three executions of NNIM-BNI are going to be reported in each examined case given the participation percentage of the three phases. Similarly to TIM-BNI, for each of the examined indicative OV LV BPL topologies of Table 1, the TIM-BNI performance assessment is going to be fulfilled through the comparison between the TIM-BNI approximated branch number value $N_{\text{NNIM}-\text{BNI}}$ and the actual one while the performance metric of RMSD will again assess the overall NNIM-BNI approximation.

In Table 2, the branch number approximations of TIM-BNI and NNIM-BNI are reported, when the aforementioned default operation settings are assumed. Apart from the branch number approximations, the actual branch numbers of the four examined OV LV BPL topologies of Table 1 are presented for comparison reasons, while the RMSDs of TIM-BNI and NNIM-BNI for the four examined OV LV BPL topologies are also computed. Note that three executions of NNIM-BNI are reported for each of the four examined OV LV BPL topologies.

From Table 2, several interesting initial remarks concerning the performance of TIM-BNI and NNIM-BNI can be pointed out. More specifically:

- With reference to the performance metric of RMSD and given the default operation settings of the base scenario, TIM-BNI seems to better approximate in general the branch number of the four indicative OV LV BPL topologies of Table 1. Indeed, the branch number approximations of TIM-BNI are closer to the actual number of branches in the cases of the urban case A, rural case and LOS case, which are anyway highlighted in green color in Table 2, in comparison with the branch number approximations of NNIM-BNI. In contrast, NNIM-BNI only better approximates the branch number of the suburban case, which is again highlighted with green color in Table 2, when 5 hidden layers are assumed.

Table 2.
Branch Number Approximations of TIM-BNI and NNIM-BNI for the Default Operation Settings

Indicative OV LV BPL Topologies of Table 1		Urban case A (Typical urban case)	Suburban case	Rural case	LOS case	RMSD	Notes
Actual Number of Branches N		3	2	1	0	-	-
TIM-BNI (Approximated Number of Branches) $N_{\text{TIM-BNI}}$		3	3	2	0.80	0.81	Default Operation Settings
NNIM-BNI (Approximated Number of Branches) $N_{\text{NNIM-BNI}}$	1st execution	2.94	2.81	2.82	2.82	1.73	Default Operation Settings + 1 hidden layer
	2nd execution	2.95	2.81	2.83	2.83	1.73	
	3nd execution	2.94	2.80	2.82	2.82	1.72	
	1st execution	8.26	1.35	2.72	2.70	3.09	Default Operation Settings + 2 hidden layers
	2nd execution	5.58	2.79	2.72	2.72	2.10	
	3nd execution	5.72	2.68	2.70	2.69	2.12	
	1st execution	2.87	2.86	2.84	2.83	1.74	Default Operation Settings + 3 hidden layers
	2nd execution	3	2.93	2.85	2.85	1.76	
	3nd execution	2.81	3.01	2.80	2.80	1.74	
	1st execution	3.01	-15.36	2.72	2.70	8.82	Default Operation Settings + 4 hidden layers
	2nd execution	2.96	-97.39	2.29	2.17	49.71	
	3nd execution	2.90	3	2.90	2.90	1.81	
	1st execution	354.21	2.15	2.06	2.19	175.61	Default Operation Settings + 5 hidden layers
	2nd execution	3.07	-159.30	2.69	2.41	80.66	
	3nd execution	3.04	-526.56	3.24	1.76	264.28	

- Since the TIM-BNI approximation of the branch number $N_{\text{TIM-BNI}}$ of each of the examined OV LV BPL topologies is equal to the average value of the branch numbers of the *5* OV LV BPL topologies of the TIM OV LV BPL topology database that present the 5 lowest RMSDs among the *P* computed ones, the TIM-BNI approximation of the branch number of the LOS case is the mean value of the LOS case, which is unique, and of four OV LV BPL topologies of one branch.

- By assuming up to 5 hidden layers and up to 3 executions per hidden layer, it is clearly shown the stochastic nature of NNIM-BNI, namely:
  - Above the third hidden layer, NNIM-BNI becomes unstable, as high or negative numbers of branches in OV LV BPL topologies are demonstrated. In fact, the differences among the NNIM-BNI branch number approximations of the different executions for given OV LV BPL topology and hidden layer are significant high, when the assumed hidden layers are above three. The previous observation is also verified by the high values of RMSD during the NNIM-BNI approximations, when the assumed hidden layers are above three.
  - When the hidden layers are below or equal to 3, RMSDs of NNIM-BNI remain low (*i.e.*, in the majority of the cases below 2) and comparable to the one of TIM-BNI (*i.e.*, 0.81). In addition, by comparing RMSD values of NNIM-BNI among the different executions, it is shown that these RMSD values remain also low and comparable among them for given number of hidden layers when hidden layers below or equal to 3 are assumed. Note that the NNIM-BNI approximations do not present negative or irrational high branch number values, when below or equal to 3 hidden layers are assumed.
- Due to the default operation settings concerning the preparation of the TIM OV LV BPL topology database, the number of OV LV BPL topologies with 3 branches is significantly higher than the number of OV LV BPL topologies with 2 branches that is again significantly higher than the number of OV LV BPL topologies with 1 branch. Note that the LOS case, which is an OV LV BPL topology with no branches, is unique. The aforementioned distribution has no impact on the performance of TIM-BNI but greatly affects the approximations and the performance of NNIM-BNI (*e.g.,* the approximation values present almost equal values, when 1 hidden layer is assumed). Therefore, the structure of the TIM OV LV BPL topology database mainly affects the NNIM-BNI performance.
- Apart from the structure of the TIM OV LV BPL topology database, the randomness during the three phases of the operation of NNIM-BNI, which comes from the participation percentages, justifies the stochastic nature of NNIM-BNI. In general, the participation percentages of the three phases of the operation of NNIM-BNI imply that different OV LV BPL topologies of the TIM OV LV BPL topology database are considered during the training of the neural networks that further affect the arrays of weights and biases of the hidden layers as denoted in eq. (6). Anyway, the NNIM-BNI approximation differences remain low, when hidden layers below or equal to 3 are assumed as it is shown among the different executions for given hidden layer number.

Apart from the operation settings of TIM-BNI and NNIM-BNI, it is obvious from the previous observations that the accuracy detail and the structure of the TIM OV LV BPL topology database critically affect the performance of both methodologies. In the following subsection, the impact of the accuracy detail and the structure of the TIM OV LV BPL topology database are assessed according to the performance of TIM-BNI and NNIM-BNI.

4.2 The Impact of TIM OV LV BPL Topology Database on TIM-BNI and NNIM-BNI Performance

In this subsection, the impact of TIM OV LV BPL topology database on the performance of TIM-BNI and NNIM-BNI is presented. First, it is evident that a more detailed TIM OV LV BPL topology may have a positive effect on the RMSDs of TIM-BNI and NNIM-BNI. Similarly to Table 2, the branch number approximations of TIM-BNI and NNIM-BNI are reported in Table 3. When the aforementioned default operation settings are assumed, but the frequency span remains equal to 1 MHz, the wider frequency range is 3-88 MHz. Apart from the branch number approximations, the actual branch numbers of the four examined OV LV BPL topologies of Table 1 and the RMSDs of TIM-BNI and NNIM-BNI for the four examined OV LV BPL topologies are presented. Again as in Table 2, three executions of NNIM-BNI are reported for each of the four examined OV LV BPL topologies.

By comparing Tables 2 and 3, the following remarks can be pointed out:

- The wider frequency range of 3-88 MHz for each of the OV LV BPL topologies of the TIM OV LV BPL topology database implies that 86 checks should occur during the operation of TIM-BNI and NNIM-BNI in Table 3 instead of the respective 28 checks of Table 2. Hence, a more rigorous approximation with higher accuracy is expected in Table 3, which is anyway reflected on the better RMSD values of both identification methods; say, the best RMSDs of TIM-BNI and NNIM-BNI are equal to 0.65 and 1.31 in Table 3 in contrast with 0.81 and 1.72 in Table 2, respectively. TIM-BNI again better approximates the branch numbers of the indicative OV LV BPL topologies in Table 3. Note that the best branch number approximation per examined OV LV BPL topology is highlighted in green color in Table 3 as well the best RMSD.

- As the branch number approximations of the four indicative OV LV BPL topologies are discussed, the higher accuracy of the TIM OV LV BPL topology database of Table 3 helps as follows:
  - NNIM-BNI accurately approximates the branch number of the urban case A. Now, TIM-BNI and NNIM-BNI can accurately identify the 3 branches of the urban case A.
  - The approximation performance of both identification methodologies remains almost the same, when the suburban case is examined.
  - Significant improvement of the approximation performance is achieved by TIM-BNI, when the rural case is investigated (*i.e.*, from 2 to 0.80 branches when the actual branch number of rural case is equal to 1). Here, it should be noted that the result of TIM-BNI is a deterministic approximation. Conversely, the accuracy performance of NNIM-BNI as reported in Table 3 remains almost the same with the one of Table 2 in the rural case.
  - As the LOS case is examined, the approximation performance of both identification methodologies remains almost the same.

- When below or equal to 3 hidden layers are examined, RMSD values of NNIM-BNI steadily remain low and comparable to the one of TIM-BNI. Anyway, for the following analysis, only one execution is going to be applied during the performance assessment of NNIM-BNI.

Table 3.
Branch Number Approximations of TIM-BNI and NNIM-BNI for the Default Operation Settings but for the Frequency Range of 3-88MHz

Indicative OV LV BPL Topologies of Table 1		Urban case A (Typical urban case)	Suburban case	Rural case	LOS case	RMSD	Notes
Actual Number of Branches N		3	2	1	0	-	-
TIM-BNI (Approximated Number of Branches) $N_{\text{TIM-BNI}}$		3	3	0.80	0.80	0.65	Default Operation Settings (Frequency Range 3-88MHz)
NNIM-BNI (Approximated Number of Branches) $N_{\text{NNIM-BNI}}$	1st execution	3	2.46	2.46	2.46	1.45	Default Operation Settings (Frequency Range 3-88MHz) + 1 hidden layer
	2nd execution	3	2.27	2.27	2.27	1.31	
	3nd execution	2.47	2.47	2.47	2.47	1.48	
	1st execution	-1894.52	-1894.01	2.70	2.38	1341.22	Default Operation Settings (Frequency Range 3-88MHz) + 2 hidden layers
	2nd execution	-338.59	-1041.68	3.47	2.47	549.08	
	3nd execution	3.28	2.89	2.73	2.72	1.68	
	1st execution	3.35	2.72	2.70	2.69	1.64	Default Operation Settings (Frequency Range 3-88MHz) + 3 hidden layers
	2nd execution	-4.47	45.72	2.73	2.71	22.23	
	3nd execution	3.13	4.20	2.65	2.48	1.86	
	1st execution	-23.31	38.16	2.61	2.52	22.41	Default Operation Settings (Frequency Range 3-88MHz) + 4 hidden layers
	2nd execution	2.99	48.46	2.90	2.10	23.27	
	3nd execution	4.46	0.71	3.46	1.90	1.83	
	1st execution	-0.21	51.89	2.76	2.25	25.04	Default Operation Settings
	2nd	6.44	3.47	2.59	2.52	2.39	

	execution						(Frequency
	3nd execution	2.47	25.95	2.62	2.37	12.06	Range 3-88MHz) + 5 hidden layers

Similarly to Table 2, RMSDs of NNIM-BNI approximations remain greater than the RMSD of TIM-BNI regardless of the number of the hidden layers and the number of executions considered. In fact, the approximated numbers of branches of suburban case, rural case and LOS case remain almost the same during the most successful NNIM-BNI approximations. This is because of the preparation of TIM OV LV BPL topology database. Due to the operation settings of TIM OV LV BPL topology database, 0.0035%, 0.19%, 4.75% and 95.05% of the OV LV BPL topologies of the TIM OV LV BPL topology database of Table 3 are OV LV BPL topologies of 0, 1, 2 and 3 branches, respectively. The aforementioned participation percentage of OV LV BPL topologies in TIM OV LV BPL topology affects the approximation performance of stochastic approximations of NNIM-BNI, thus explaining the almost equal approximated numbers of branches of the suburban case, rural case and LOS case.

Although the performance of both identification methodologies significantly depends on the accuracy degree of the TIM OV LV BPL topology database as shown in Table 3, the RMSD values can get improved even more especially in the cases of the stochastic NNIM-BNI approximations, when representative sets of the TIM OV LV BPL topology database are applied. A good representative set should capture the most information from the original TIM OV LV BPL topology database [58]. Algorithms (such as Maximum Coverage, k-medoid clustering, etc [59, 60]) can generate balanced subsets that capture original information from the initial TIM OV LV BPL topology database. Here, three representative sets of the TIM OV LV BPL topology database of Table 3 are applied, where the number of OV LV BPL topologies of 1, 2 and 3 branches remains the same in the representative sets. The selection of OV LV BPL topologies with 2 and 3 branches is random among the available ones from the TIM OV LV BPL topology database of Table 3. In Table 4, the branch number approximations of TIM-BNI and NNIM-BNI are reported, when the aforementioned default operation settings of Sec.4.1 are assumed but for three representative sets of the TIM OV LV BPL topology database of Table 3. Apart from the branch number approximations, the actual branch numbers of the four examined OV LV BPL topologies of Table 1 are again presented. Also, RMSDs of TIM-BNI and NNIM-BNI for the four examined OV LV BPL topologies are demonstrated. Note that the three representative sets consist of random OV LV BPL topologies of 2 and 3 branches from the initial TIM OV LV BPL topology database, so the different deterministic TIM-BNI and stochastic NNIM-BNI approximations are expected in Table 4.

Table 4.
Branch Number Approximations of TIM-BNI and NNIM-BNI for the Default Operation Settings but for
Frequency Range 3-88MHz and Three Representative Sets of OV LV BPL Topologies from the
TIM OV LV BPL Topology Database

Indicative OV LV BPL Topologies of Table 1		Urban case A (Typical urban case)	Suburban case	Rural case	LOS case	RMSD	Notes
Actual Number of Branches N		**3**	**2**	**1**	**0**	-	-
TIM-BNI (Approximated Number of Branches) $N_{\text{TIM-BNI}}$	1st representative set	2.40	2.20	0.80	0.80	0.52	Default Operation Settings (Frequency Range 3-88MHz + Representative Sets)
	2nd representative set	3	2.80	0.80	0.80	0.57	
	3rd representative set	2.60	2.40	0.80	0.80	0.50	
NNIM-BNI (Approximated Number of Branches) $N_{\text{NNIM-BNI}}$	1st representative set	2.46	1.76	1.57	1.56	0.88	Default Operation Settings (Frequency Range 3-88MHz + Representative Sets) + 1 hidden layer
	2nd representative set	3.42	2	0.99	0.94	0.52	
	3rd representative set	3.59	1.81	1.06	1.01	0.590	
	1st representative set	14.32	1.10	1.07	0.650	5.69	Default Operation Settings (Frequency Range 3-88MHz + Representative Sets) + 2 hidden layers
	2nd representative set	1.94	1.85	1.85	1.84	1.15	
	3rd representative set	3.83	2.09	0.930	0.870	0.61	
	1st representative set	2.92	1.95	1.03	0.980	0.490	Default Operation Settings (Frequency Range 3-88MHz + Representative Sets) + 3 hidden layers
	2nd representative set	2.02	2.02	2.02	2.02	1.23	
	3rd representative set	3.05	2.03	1.06	1.03	0.52	
	1st representative set	4.77	2.77	1	0.920	1.07	Default Operation Settings (Frequency
	2nd	2.93	1.94	1.30	1.29	0.66	

	representative set						Range 3-88MHz + Representative Sets) + 4 hidden layers
	3nd representative set	2.45	1.81	1.37	1.36	0.76	
	1st representative set	1.60	1.68	1.83	1.84	1.24	Default Operation Settings (Frequency Range 3-88MHz + Representative Sets) + 5 hidden layers
	2nd representative set	3.56	5.62	1	0.68	1.86	
	3nd representative set	5.64	2.24	1.01	0.94	1.41	

By comparing Tables 2-4, it is clear that the approximation performances of TIM-BNI and NNIM-BNI have significantly been improved, while RMSDs of NNIM-BNI become comparable to the ones of TIM-BNI. Indeed, the best RMSDs of TIM-BNI and NNIM-BNI after the selection of representative sets from the TIM OV LV BPL topology database of Table 3 are equal to 0.50 and 0.52, respectively, which are the best RMSDs among the Tables 2, 3 and 4. Among the indicative OV LV BPL topologies of Table 1, TIM-BNI better approximates the branches of urban case A (*i.e.*, the best TIM-BNI approximation is equal to 3, while the actual number of branches is equal to 3), whereas NNIM-NMI better approximates the branches of suburban, rural and LOS case A (*i.e.*, the best NNIM-BNI approximations are equal to 2, 1 and 0.68 when the actual numbers of branches are equal to 2, 1 and 0, respectively). In addition, the representative sets from the TIM OV LV BPL topology database first differentiate the NNIM-BNI approximations among the suburban rural and LOS cases and second improve the NNIM-BNI performance, when high number of hidden layers are applied. Note that the best branch number approximation per examined OV LV BPL topology is highlighted in green color in Table 4 as well the best RMSD. In general, the findings of this subsection highlight the problem of AI bias while the representative sets can define cleaner datasets from conscious or unconscious prejudices thus allowing more accurate approximations.

In this subsection, the performance improvement of TIM-BNI and NNIM-BNI has been highlighted when: (i) higher accuracies for the preparation of TIM OV LV BPL topology database, and (ii) representative sets depending on the examined indicative OV LV BPL topologies are applied. Apart from the impact of more sophisticated TIM OV LV BPL topology databases on TIM-BNI and NNIM-BNI performance, significant improvement can be achieved when the operation settings of TIM-BNI (*i.e.*, see Sec.4.3) and NNIM-BNI (*i.e.*, see Sec.4.4) are further explored as follows.

4.3 The Impact of *R* on TIM-BNI Performance
Apart from the operation settings that affect the preparation of the TIM OV LV BPL topology database and, thus, the performance of TIM-BNI and NNIM-BNI,

the operation settings of TIM-BNI that affect its approximation performance is studied in this subsection.

As already been mentioned in Sec. 3.1, the TIM-BNI branch number approximation $N_{\mathrm{TIM-BNI}}$ comes from the average value of the branch numbers of the R OV LV BPL topologies of the TIM OV LV BPL topology database, which presents the R lowest RMSDs among the P computed ones, while the default value of R is equal to 5. In Table 5, the branch number approximations of TIM-BNI are reported, when the aforementioned default operation settings of Sec.4.1 are assumed but for six different values of R (i.e, 1, 2, 3, 5, 7 and 10). Apart from the branch number approximations, the actual branch numbers of the four examined OV LV BPL topologies of Table 1 are again presented. Also, RMSDs of TIM-BNI for the four examined OV LV BPL topologies and the six different values of R are demonstrated.

From Table 5, it is evident that RMSD depends on the value of R. As the TIM-BNI branch number approximations of urban case A, suburban case and rural case do not depend on the value of R, RMSD is only affected by the branch number approximation of LOS case. Since the LOS case is unique in the TIM OV LV BPL topology database, when R increases, this implies that (R-1) OV LV BPL topologies of the TIM OV LV BPL topology database of different number of branches but with the (R-1) lowest RMSDs are taken into account during the computation of the average of branch numbers. Therefore, as R increases, the number of approximate branches in the LOS case will also increase. Note that the best branch number approximation per examined OV LV BPL topology and the best RMSD are highlighted in green color in Table 5.

4.4 The Impact of Participation Percentages on NNIM-BNI Performance

Until now, the operation settings that affect the preparation of the TIM OV LV BPL topology database and the operation of TIM-BNI have been studied. In this subsection, the factors that affect the approximation performance of NNIM-BNI are analyzed. More specifically, the main factor that affects the operation of NNIM-BNI is the participation percentages of the three phases, *i.e.*, training, validation and testing. In Table 6, the branch number approximations of NNIM-BNI are reported, when the aforementioned default operation settings of Sec.4.1 are assumed but for seven participation percentage combinations –*i.e.*, (10%,45%,45%), (30%,35%,35%), (50%,25%,25%), (70%,15%,15%), (80%,10%,10%), (80%,10%,10%), (90%,5%,5%) and (98%,1%,1%)–. Apart from the branch number approximations, the actual branch numbers of the four examined OV LV BPL topologies of Table 1 are again presented. Also, RMSDs of TIM-BNI for the four examined OV LV BPL topologies and the seven different participation percentage combinations are demonstrated. Note that up to 5 hidden layers and one execution per hidden layer and participation percentage combination are assumed in Table 6.

Table 5.
Branch Number Approximations of TIM-BNI for the Default Operation Settings and Different *R* Values

Indicative OV LV BPL Topologies of Table 1		Urban case A (Typical urban case)	Suburban case	Rural case	LOS case	RMSD	Notes
Actual Number of Branches *N*		3	2	1	0	-	-
TIM-BNI (Approximated Number of Branches) $N_{\text{TIM-BNI}}$	*R*=1	3	3	2	0	0.71	Default Operation Settings
	R=2	3	3	2	0.50	0.75	
	R=3	3	3	2	0.67	0.78	
	R=5 (Default)	3	3	2	0.80	0.81	
	R=7	3	3	2	1	0.87	
	R=10	3	3	2	1.30	0.96	

Table 6.
Branch Number Approximations of NNIM-BNI for the Default Operation Settings and Different Participation Percentage Values of Training, Validation and Testing

Indicative OV LV BPL Topologies of Table 1		Urban case A (Typical urban case)	Suburban case	Rural case	LOS case	RMSD	Notes
Actual Number of Branches *N*		3	2	1	0	-	-
	Participation Percentages for Training, Validation and Testing (%,%,%)						
NNIM-BNI (Approximated Number of Branches) $N_{\text{NNIM-BNI}}$	(10%,45%,45%)	2.94	2.94	2.94	2.94	1.82	Default Operation Settings + 1 hidden layer
	(30%,35%,35%)	3.07	2.83	2.62	2.59	1.58	
	(50%,25%,25%)	2.41	2.41	2.41	2.41	1.44	
	(70%,15%,15%) Default	2.94	2.81	2.82	2.82	1.73	
	(80%,10%,10%)	3	2.49	2.49	2.49	1.47	
	(90%,5%,5%)	3.06	2.86	2.77	2.76	1.70	
	(98%,1%,1%)	3	3	2.55	2.55	1.58	
	(10%,45%,45%)	5.03	2.82	2.58	2.52	1.85	Default Operation Settings + 2 hidden layers
	(30%,35%,35%)	4.96	3.33	2.61	2.52	1.91	
	(50%,25%,25%)	5.71	3.44	2.53	2.44	2.10	
	(70%,15%,15%) Default	8.26	1.35	2.72	2.70	3.09	
	(80%,10%,10%)	5.58	3.47	2.61	2.56	2.12	
	(90%,5%,5%)	-51.36	54.23	2.60	2.53	37.72	
	(98%,1%,1%)	759.24	3.02	2.77	1.57	378.12	

(10%,45%,45%)	6.15	6.14	2.56	2.40	2.97	Default Operation Settings + 3 hidden layers
(30%,35%,35%)	2.98	3.35	2.47	2.23	1.50	
(50%,25%,25%)	3.18	2.81	2.51	2.41	1.48	
(70%,15%,15%) Default	2.87	2.86	2.84	2.83	1.74	
(80%,10%,10%)	5.40	3.39	2.61	2.56	2.05	
(90%,5%,5%)	-0.250	0.40	2.93	2.66	2.45	
(98%,1%,1%)	3.89	3.07	2.64	2.61	1.69	
(10%,45%,45%)	4.82	0.99	2.55	2.45	1.78	Default Operation Settings + 4 hidden layers
(30%,35%,35%)	2.21	5.93	2.51	2.36	2.44	
(50%,25%,25%)	5.73	3.50	2.62	2.56	2.17	
(70%,15%,15%) Default	3.01	-15.36	2.72	2.70	8.82	
(80%,10%,10%)	4.72	3.43	2.62	2.58	1.89	
(90%,5%,5%)	4.89	3.24	2.61	2.58	1.90	
(98%,1%,1%)	2.98	2.87	2.87	2.86	1.76	
(10%,45%,45%)	3.65	2.90	2.64	2.62	1.64	Default Operation Settings + 5 hidden layers
(30%,35%,35%)	4.38	2.87	2.63	2.58	1.73	
(50%,25%,25%)	3.01	2.01	2.64	2.57	1.52	
(70%,15%,15%) Default	354.21	2.15	2.06	2.19	175.61	
(80%,10%,10%)	2.24	1.63	2.71	2.49	1.57	
(90%,5%,5%)	3	3	3.48	2.41	1.80	
(98%,1%,1%)	5.50	3.51	2.59	2.55	2.09	

From Table 6, the significance of the validation and testing phases is outlined, since low RMSDs can be detected when high participation percentages of the previous phases (*i.e.*, above 15%) are assumed regardless of the number of hidden layers. Indeed, the highest RMSDs occurring are equal to 378.1 and 175.61, when participation percentage of validation phase is equal to 1% and 15%, respectively. Note that the lowest RMSD that is equal to 1.44 occurs, when one hidden layer is applied and the participation percentages for training, validation and testing are equal to 50%, 25% and 25%, respectively. Finally, 1 and 3 hidden layers offer more secure approximations regardless of the participation percentage combinations, since in all the other numbers of hidden layers, there is at least one participation percentage combination whose RMSD is above 5 renders inacceptable an approximation. Note that the best branch number approximation per examined OV LV BPL topology is highlighted in green color in Table 6 as well the best RMSD.

Concluding this Section, the approximation performance impact of a variety of settings that affects the preparation of the TIM OV LV BPL topology database and the operation of TIM-BNI and NNIM-BNI has been assessed. The factors that affect the preparation of the TIM OV LV BPL topology database, such as its accuracy degree and its representativeness, has the most significant effect on the approximation performance of TIM-BNI and NNIM-BNI thus rendering NNIM-BNI equivalent to TIM-BNI. On the basis of the factors that affect the accuracy degree of the TIM OV LV BPL topology database, the effect of lower values of the length spacing L_s for both branch distance and branch length and of higher values of the maximum branch length $L_{b,max}$ during the preparation of the TIM OV LV BPL topology database on the approximation performance of NNIM-BNI is as subject of future research.

5. Conclusions

In this paper, the branch number approximation methods of TIM-BNI and NNIM-BNI have been proposed, while the factors that affect their approximation performance have been recognized and benchmarked. The factors that affect the preparation of the TIM OV LV BPL topology database, which is the big data input of TIM-BNI and NNIM-BNI, have a significant impact on their approximation performance; the accuracy degree and the representativeness of the TIM OV LV BPL topology database have significantly improved RMSDs of the branch number approximations of both TIM-BNI and NNIM-BNI. As the operation settings of TIM-BNI are concerned, it has been revealed that the least the number of OV LV BPL topologies of the TIM OV LV BPL topology database are taken into account during the deterministic TIM-BNI branch number approximation, the better the RMSDs of the TIM-BNI approximations get. As the operation settings of NNIM-BNI are regarded, the hidden layers and the participation percentages of training, validation and testing may affect the stochastic NNIM-BNI branch number approximations. In fact, the best approximation performances with reference to RMSD have been reported when below three hidden layers and high participation percentages of the validation and testing phases are assumed. In the future research steps, TIM-BNI and NNIM-BNI are going to be further elaborated and expanded in order to cope with the fervent issues of the operation of the smart grid.

CONFLICTS OF INTEREST

The author declares that there is no conflict of interests regarding the publication of this paper.

References

[1]   F. Aalamifar and L. Lampe, "Optimized WiMAX profile configuration for smart grid communications," *IEEE Transactions on Smart Grid*, vol. 8, no. 6, pp. 2723-2732, 2017.

[2]   A. G. Lazaropoulos, "Wireless Sensor Network Design for Transmission Line Monitoring, Metering and Controlling Introducing Broadband over PowerLines-enhanced Network Model (BPLeNM)," *ISRN Power Engineering*, vol. 2014, Article ID 894628, 22 pages, 2014. doi:10.1155/2014/894628. [Online]. Available:
http://www.hindawi.com/journals/isrn.power.engineering/2014/894628/

[3]   A. G. Lazaropoulos, "Improvement of Power Systems Stability by Applying Topology Identification Methodology (TIM) and Fault and Instability Identification Methodology (FIIM)–Study of the Overhead Medium-Voltage Broadband over Power Lines (OV MV BPL) Networks Case," *Trends in*

Renewable Energy, vol. 3, no. 2, pp. 102-128, Apr. 2017. [Online]. Available: http://futureenergysp.com/index.php/tre/article/view/34

[4]   A. G. Lazaropoulos, "Main Line Fault Localization Methodology in Smart Grid–Part 1: Extended TM2 Method for the Overhead Medium-Voltage Broadband over Power Lines Networks Case," *Trends in Renewable Energy*, vol. 3, no. 3, pp. 2-25, Dec. 2017. [Online]. Available: http://futureenergysp.com/index.php/tre/article/view/36

[5]   A. G. Lazaropoulos, "Business Analytics and IT in Smart Grid – Part 1: The Impact of Measurement Differences on the iSHM Class Map Footprints of Overhead Low-Voltage Broadband over Power Lines Topologies," *Trends in Renewable Energy*, vol. 6, no. 2, pp. 156-186, May 2020. [Online]. Available: http://futureenergysp.com/index.php/tre/article/view/117/pdf

[6]   M. H. Rehmani, M. Reisslein, A. Rachedi, M. Erol-Kantarci, and M. Radenkovic, "Integrating renewable energy resources into the smart grid: recent developments in information and communication technologies," *IEEE Transactions on Industrial Informatics*, vol. 14, no. 7, pp. 2814-2825, 2018.

[7]   F. R. Yu, P. Zhang, W. Xiao, and P. Choudhury, "Communication systems for grid integration of renewable energy resources," *IEEE Network*, vol. 25, no. 5, pp. 22–29, Sep. 2011.

[8]   B. Heile, "Smart grids for green communications [industry perspectives]," *IEEE Wireless Commun.*, vol. 17, no. 3, pp. 4–6, Jun. 2010.

[9]   A. G. Lazaropoulos, "Review and Progress towards the Capacity Boost of Overhead and Underground Medium-Voltage and Low-Voltage Broadband over Power Lines Networks: Cooperative Communications through Two- and Three-Hop Repeater Systems," *ISRN Electronics*, vol. 2013, Article ID 472190, pp. 1-19, 2013. [Online]. Available: http://www.hindawi.com/isrn/electronics/aip/472190/

[10]   A. S. de Beer, A. Sheri, H. C. Ferreira, and A. H. Vinck, "Channel frequency response for a low voltage indoor cable up to 1GHz," In *Power Line Communications and its Applications (ISPLC), 2018 IEEE International Symposium on*, pp. 1-6, 2018.

[11]   A. G. Lazaropoulos and P. G. Cottis, "Transmission characteristics of overhead medium voltage power line communication channels," *IEEE Trans. Power Del.*, vol. 24, no. 3, pp. 1164-1173, Jul. 2009.

[12]   A. G. Lazaropoulos and P. G. Cottis, "Capacity of overhead medium voltage power line communication channels," *IEEE Trans. Power Del.*, vol. 25, no. 2, pp. 723-733, Apr. 2010.

[13]   A. G. Lazaropoulos and P. G. Cottis, "Broadband transmission via underground medium-voltage power lines-Part I: transmission characteristics," *IEEE Trans. Power Del.*, vol. 25, no. 4, pp. 2414-2424, Oct. 2010.

[14]   A. G. Lazaropoulos and P. G. Cottis, "Broadband transmission via underground medium-voltage power lines-Part II: capacity," *IEEE Trans. Power Del.*, vol. 25, no. 4, pp. 2425-2434, Oct. 2010.

[15]   E. Biglieri, "Coding and modulation for a horrible channel," *IEEE Commun. Mag.*, vol. 41, no. 5, pp. 92–98, May 2003.

[16]   M. Gebhardt, F. Weinmann, and K. Dostert, "Physical and regulatory constraints for communication over the power supply grid," *IEEE Commun. Mag.*, vol. 41, no. 5, pp. 84-90, May 2003.

[17]   P. S. Henry, "Interference characteristics of broadband power line communication systems using aerial medium voltage wires," *IEEE Commun. Mag.*, vol. 43, no. 4, pp. 92-98, Apr. 2005.

[18]   S. Liu and L. J. Greenstein, "Emission characteristics and interference constraint of overhead medium-voltage broadband power line (BPL) systems," in *Proc. IEEE Global Telecommunications Conf.*, New Orleans, LA, USA, Nov./Dec. 2008, pp. 1-5.

[19]   M. Götz, M. Rapp, and K. Dostert, "Power line channel characteristics and their effect on communication system design," *IEEE Commun. Mag.*, vol. 42, no. 4, pp. 78-86, Apr. 2004.

[20]   A. G. Lazaropoulos, "Towards Modal Integration of Overhead and Underground Low-Voltage and Medium-Voltage Power Line Communication Channels in the Smart Grid Landscape: Model Expansion, Broadband Signal Transmission Characteristics, and Statistical Performance Metrics (Invited Paper)," *ISRN Signal Processing*, vol. 2012, Article ID 121628, pp. 1-17, 2012. [Online]. Available: http://www.hindawi.com/isrn/sp/2012/121628/

[21]   D. G. Della and S. Rinaldi, "Hybrid Communication Network for the Smart Grid: Validation of a Field Test Experience," *IEEE Trans. Power Del.*, vol. 30, no. 6, pp. 2492-2500, 2015.

[22]   F. Versolatto and A. M. Tonello, "An MTL theory approach for the simulation of MIMO power-line communication channels," *IEEE Trans. Power Del.*, vol. 26, no. 3, pp. 1710-1717, Jul. 2011.

[23]   P. Amirshahi and M. Kavehrad, "High-frequency characteristics of overhead multiconductor power lines for broadband communications," *IEEE J. Sel. Areas Commun.*, vol. 24, no. 7, pp. 1292-1303, Jul. 2006.

[24]   L. Stadelmeier, D. Schneider, D. Schill, A. Schwager, and J. Speidel, "MIMO for inhome power line communications," presented at the *Int. Conf. on Source and Channel Coding*, Ulm, Germany, Jan. 2008.

[25]   T. Sartenaer, "Multiuser communications over frequency selective wired channels and applications to the powerline access network" *Ph.D. dissertation*, Univ. Catholique Louvain, Louvain-la-Neuve, Belgium, Sep. 2004.

[26]   T. Calliacoudas and F. Issa, ""Multiconductor transmission lines and cables solver," An efficient simulation tool for plc channel networks development," presented at the *IEEE Int. Conf. Power Line Communications and Its Applications*, Athens, Greece, Mar. 2002.

[27]   S. Galli and T. Banwell, "A deterministic frequency-domain model for the indoor power line transfer function," *IEEE J. Sel. Areas Commun.*, vol. 24, no. 7, pp. 1304-1316, Jul. 2006.

[28]   S. Galli and T. Banwell, "A novel approach to accurate modeling of the indoor power line channel-Part II: Transfer function and channel properties," *IEEE Trans. Power Del.*, vol. 20, no. 3, pp. 1869-1878, Jul. 2005.

[29]   A. Pérez, A. M. Sánchez, J. R. Regué, M. Ribó, R. Aquilué, P. Rodréguez-Cepeda, and F. J. Pajares, "Circuital and modal characterization of the power-line network in the PLC band," *IEEE Trans. Power Del.*, vol. 24, no. 3, pp. 1182-1189, Jul. 2009.

[30]   T. Sartenaer and P. Delogne, "Deterministic modelling of the (Shielded) outdoor powerline channel based on the multiconductor transmission line equations," *IEEE J. Sel. Areas Commun.*, vol. 24, no. 7, pp. 1277-1291, Jul. 2006.

[31] T. Sartenaer and P. Delogne, "Powerline cables modelling for broadband communications," in Proc. *IEEE Int. Conf. Power Line Communications and Its Applications*, Malmö, Sweden, Apr. 2001, pp. 331-337.

[32] C. R. Paul, *Analysis of Multiconductor Transmission Lines*. New York: Wiley, 1994.

[33] J. A. B. Faria, *Multiconductor Transmission-Line Structures: Modal Analysis Techniques*. New York: Wiley, 1994.

[34] H. Meng, S. Chen, Y. L. Guan, C. L. Law, P. L. So, E. Gunawan, and T. T. Lie, "Modeling of transfer characteristics for the broadband power line communication channel," *IEEE Trans. Power Del.*, vol. 19, no. 3, pp. 1057-1064, Jul. 2004.

[35] A. Semlyen and B. Gustavsen, "Phase-domain transmission-line modeling with enforcement of symmetry via the propagated characteristic admittance matrix," *IEEE Trans. Power Del.*, vol. 27, no. 2, pp. 626-631, Apr. 2012.

[36] A. G. Lazaropoulos, "Statistical Broadband over Power Lines Channel Modeling – Part 1: The Theory of the Statistical Hybrid Model," *Progress in Electromagnetics Research C*, vol. 92, pp. 1-16, 2019. [Online]. Available: http://www.jpier.org/PIERC/pierc92/01.19012902.pdf

[37] A. G. Lazaropoulos, "Measurement Differences, Faults and Instabilities in Intelligent Energy Systems – Part 2: Fault and Instability Prediction in Overhead High-Voltage Broadband over Power Lines Networks by Applying Fault and Instability Identification Methodology (FIIM)," *Trends in Renewable Energy*, vol. 2, no. 3, pp. 113-142, Oct. 2016. [Online]. Available: http://futureenergysp.com/index.php/tre/article/view/27/33

[38] A. G. Lazaropoulos, "Measurement Differences, Faults and Instabilities in Intelligent Energy Systems–Part 1: Identification of Overhead High-Voltage Broadband over Power Lines Network Topologies by Applying Topology Identification Methodology (TIM)," *Trends in Renewable Energy*, vol. 2, no. 3, pp. 85-112, Oct. 2016. [Online]. Available: http://futureenergysp.com/index.php/tre/article/view/26/32

[39] Y. Huo, G. Prasad, L. Lampe, and V. C. Leung, "Advanced Smart Grid Monitoring: Intelligent Cable Diagnostics using Neural Networks," in *Proc. IEEE Int. Symp. Power Line Communications and its Applications*, May 2020, pp. 1-6.

[40] A. M. Tonello, N. A. Letizia, D. Righini, and F. Marcuzzi, "Machine learning tips and tricks for power line communications," *IEEE Access*, vol. 7, pp. 82434-82452, 2019.

[41] Y. Cui, X. Liu, J. Cao, and D. Xu, "Network Performance Optimization for Low-Voltage Power Line Communications," *MDPI Energies*, vol. 11, no. 5, pp. 1266-1290, 2018.

[42] M. Ibnkahla, "Applications of neural networks to digital communications–a survey. Signal processing," vol. 80, no. 7, pp. 1185-1215, 2020.

[43] D. Okoh, *Computer Neural Networks on MATLAB*. CreateSpace Independent Publishing Platform, 2016.

[44] K. P. Murphy, *Machine Learning: A Probabilistic Perspective*. Cambridge, MA, USA: MIT Press, 2012.

[45] A. G. Lazaropoulos, "Statistical Channel Modeling of Overhead Low Voltage Broadband over Power Lines (OV LV BPL) Networks – Part 1: The Theory of Class Map Footprints of Real OV LV BPL Topologies, Branch Line Faults and Hook-Style Energy Thefts," *Trends in Renewable Energy*, vol. 6, no. 1, pp. 61-87,

Mar.   2020.   [Online].   Available:
http://futureenergysp.com/index.php/tre/article/download/112/pdf

[46]   OPERA1, D44: Report presenting the architecture of plc system, the electricity network topologies, the operating modes and the equipment over which PLC access system will be installed, IST Integr. Project No 507667, Dec. 2005.

[47]   P. Amirshahi, "Broadband access and home networking through powerline networks" Ph.D. dissertation, Pennsylvania State Univ., University Park, PA, May 2006.

[48]   M. D'Amore and M. S. Sarto, "A new formulation of lossy ground return parameters for transient analysis of multiconductor dissipative lines," *IEEE Trans. Power Del.*, vol. 12, no. 1, pp. 303-314, Jan. 1997.

[49]   M. D'Amore and M. S. Sarto, "Simulation models of a dissipative transmission line above a lossy ground for a wide-frequency range-Part I: Single conductor configuration," *IEEE Trans. Electromagn. Compat.*, vol. 38, no. 2, pp. 127-138, May 1996.

[50]   M. D'Amore and M. S. Sarto, "Simulation models of a dissipative transmission line above a lossy ground for a wide-frequency range-Part II: Multi-conductor configuration," *IEEE Trans. Electromagn. Compat.*, vol. 38, no. 2, pp. 139-149, May 1996.

[51]   A. G. Lazaropoulos, "Broadband Performance Metrics and Regression Approximations of the New Coupling Schemes for Distribution Broadband over Power Lines (BPL) Networks," *Trends in Renewable Energy*, vol. 4, no. 1, pp. 43-73,   Jan.   2018.   [Online].   Available:
http://futureenergysp.com/index.php/tre/article/view/59/pdf

[52]   A. G. Lazaropoulos, "New Coupling Schemes for Distribution Broadband over Power Lines (BPL) Networks," *Progress in Electromagnetics Research B*, vol. 71,   pp.   39-54,   2016.   [Online].   Available:
http://www.jpier.org/PIERB/pierb71/02.16081503.pdf

[53]   I. C. Demetriou, "An application of best *L*1 piecewise monotonic data approximation to signal restoration," *IAENG International Journal of Applied Mathematics*, vol. 53, no. 4, pp. 226-232, 2013.

[54]   I. C. Demetriou, "L1PMA: A Fortran 77 Package for Best L1 Piecewise Monotonic Data Smoothing," *Computer Physics Communications*, vol. 151, no. 1, pp. 315-338, 2003.

[55]   Y. T. Ma, K. H. Liu, and Y. N. Guo, "Artificial neural network modeling approach to power-line communication multi-path channel," in *Proc. Int. Conf. Neural Netw. Signal Process*, Jun. 2008, pp. 229-232.

[56]   R. Hecht-Nielsen, "Theory of the backpropagation neural network," *Neural networks for perception. Academic Press*, pp. 65-93, 1992.

[57]   D.   Okoh,   Neural   Network   Training   Code
(https://www.mathworks.com/matlabcentral/fileexchange/59362-neural-network-training-code), MATLAB Central File Exchange. Retrieved April 22, 2020.

[58]   F. Pan, W. Wang, A. K. Tung, and J. Yang, "Finding representative set from massive data," In *Fifth IEEE International Conference on Data Mining (ICDM'05)*, Nov. 2005.

[59]   S. V. R. Kannan and A. Veta, "On clusterings: Good, bad and spectral," *Journal of the ACM (JACM)*, vol. 51, no. 3, pp. 497-515, 2000.

[60]   D. S. Hochbaum and A. Pathria, "Analysis of the greedy approach in problems of maximum k-coverage," *Naval Research Quarterly*, vol. 45, pp. 615-627, 1998.